



HAL
open science

Specific expression patterns and cell distribution of ancient and modern PAG in bovine placenta during pregnancy

Eve Touzard Touzard, Pierrette P. Renaud, Olivier O. Dubois, Catherine C. Guyader-Joly, Patrice P. Humblot, Claire C. Ponsart, Gilles Charpigny

► To cite this version:

Eve Touzard Touzard, Pierrette P. Renaud, Olivier O. Dubois, Catherine C. Guyader-Joly, Patrice P. Humblot, et al.. Specific expression patterns and cell distribution of ancient and modern PAG in bovine placenta during pregnancy. *Reproduction*, 2013, 146 (4), pp.347-362. 10.1530/REP-13-0143 . hal-01004079

HAL Id: hal-01004079

<https://hal.science/hal-01004079>

Submitted on 29 May 2020

HAL is a multi-disciplinary open access archive for the deposit and dissemination of scientific research documents, whether they are published or not. The documents may come from teaching and research institutions in France or abroad, or from public or private research centers.

L'archive ouverte pluridisciplinaire **HAL**, est destinée au dépôt et à la diffusion de documents scientifiques de niveau recherche, publiés ou non, émanant des établissements d'enseignement et de recherche français ou étrangers, des laboratoires publics ou privés.

Specific expression patterns and cell distribution of ancient and modern PAG in bovine placenta during pregnancy

Eve Touzard^{1,2}, Pierrette Reinaud¹, Olivier Dubois¹, Catherine Guyader-Joly², Patrice Humblot³, Claire Ponsart² and Gilles Charpigny¹

¹INRA, UMR1198, Biologie du Développement et Reproduction, F-78352 Jouy-en-Josas, France, ²UNCEIA, Union Nationale des Coopératives d'Élevage et d'Insémination Animale, Recherche et Développement, F-94704 Maisons-Alfort, France and ³SLU, Department of Clinical Sciences, Faculty of Veterinary Medicine and Animal Science, Swedish University of Agricultural Sciences, SE 750 07 Uppsala, Sweden

Correspondence should be addressed to G Charpigny who is now at INRA, Domaine de Vilvert, UMR1198, Biologie du Développement et Reproduction, 78350 Jouy-En-Josas, France; Email: gilles.charpigny@jouy.inra.fr

Abstract

Pregnancy-associated glycoproteins (PAGs) constitute a multigenic family of aspartic proteinases expressed in the trophoblast of the ruminant placenta. In *Bos taurus*, this family comprises 21 members segregated into ancient and modern phylogenetic groups. Ancient PAGs have been reported to be synthesized throughout the trophoblastic cell layer whereas modern PAGs are produced by binucleate cells of cotyledons. The aim of this study was to investigate modern and ancient PAGs during gestation in cotyledonary and intercotyledonary tissues. To obtain convincing and innovative results despite the high sequence identity shared between PAGs, we designed specific tools such as amplification primers and antibodies. Using real-time RT-PCR, we described the transcript expression of 16 bovine PAGs. Overall, PAGs are characterized by an increase in their expression during gestation. However, we demonstrated a segregation of modern PAGs in cotyledons and of ancient PAGs in the intercotyledonary chorion, except for the ancient PAG2 expressed in cotyledons. By raising specific antibodies against the modern PAG1 and ancient PAG11 and PAG2, we established the expression kinetics of the proteins using western blotting. Immunohistochemistry showed that PAGs were produced by specific cellular populations: PAG1 by binucleate cells in the whole trophoblastic layer, PAG11 was localized in binucleate cells of the intercotyledonary trophoblast and the chorionic plate of the cotyledon, while PAG2 was produced in mononucleate cells of the internal villi of the cotyledon. These results revealed a highly specific regulation of PAG expression and cell localization as a function of their phylogenetic status, suggesting distinct biological functions within placental tissues.

Reproduction (2013) **146** 347–362

Introduction

The ruminant placenta is characterized by specific structural and functional features: the placentomes. These structures are discrete areas of massive interdigitations between the maternal endometrium and the foetal chorioallantois, which facilitate communication and exchanges between the foetal and maternal compartments. The placentome combines embryonic and maternal villi called cotyledon and caruncle respectively. The external surface of the placenta is a single-cell layer, the trophoblast, which covers the cotyledonary and intercotyledonary areas. The trophoblast is made up of two different cell types: mononucleate cells that account for 80% of the total trophoblastic population and binucleate cells (Wooding & Wathes 1980, Wooding 1983). Mononucleate cells play a fundamental role in the maternal recognition of pregnancy via the secretion of interferon- τ and in foetal nutrition via the

absorption of uterine histotroph. Binucleate cells have been suspected as being involved in conceptus implantation and are essential to the maintenance of pregnancy via their endocrine function (Igwebuike 2006). Among the molecules produced by trophoblastic cells, the pregnancy-associated glycoprotein (PAG) multigenic family represents a set of proteins that is synthesized in the whole cellular layer (Zoli *et al.* 1992, Xie *et al.* 1994, Green *et al.* 2000). In *Bos taurus*, 21 PAG genes and 20 PAG-like genes have been identified in GENBANK (<http://www.ncbi.nlm.nih.gov/nucleotide/>). PAGs are proteins whose molecular weights range from 37 to 90 kDa (Butler *et al.* 1982, Xie *et al.* 1991, 1994, Zoli *et al.* 1991, Szafranska *et al.* 2006). They belong to the large family of aspartic proteinases. However, the function of PAG remains unknown. Hypotheses concerning the modulation of immune activity (Dosogne *et al.* 1999, 2000) and the maintenance of

pregnancy (Weems *et al.* 1998, 1999, 2001, Bridges *et al.* 1999, Thompson *et al.* 2012) have been investigated to date.

Phylogenetic studies have shown that PAGs segregate into one ancient group and a more recent group (Green *et al.* 2000, Hughes *et al.* 2000). The latter refers to modern molecules that appeared about 52 millions years ago, whereas the ancient group includes members that have probably existed for about 87 millions years. Modern PAGs, typified by PAG1, have been extensively characterized and are known to be synthesized in binucleate cells of the cotyledon (Xie *et al.* 1991, Zoli *et al.* 1992, Green *et al.* 1998, Wooding *et al.* 2005). In contrast, ancient PAGs (PAG2, PAG8, PAG10, PAG11, PAG12 and PAG13) have been poorly described. According to earlier studies, ancient PAGs were reported to be expressed throughout the trophoblastic cell layer (Xie *et al.* 1994, Green *et al.* 2000) or at the junction between the cotyledonary trophoblast and caruncular endometrium (Wooding *et al.* 2005). Doubt remains regarding the reliability and accuracy of the data available on the location and expression of PAGs in the ancient group. Because modern PAGs have been widely used as pregnancy markers to detect gravid cows, considerable attention has been paid to describing PAGs in the maternal circulation (Sasser *et al.* 1986, Mialon *et al.* 1993). Many other studies have focused on the characterization of PAGs in the cotyledon (Xie *et al.* 1991, Klisch & Leiser 2003, Wooding *et al.* 2005, Telugu *et al.* 2009) as the principal placental region that produces modern PAGs for delivery into the maternal blood flow. There is relevant evidence in favour of PAG expression in the intercotyledonary chorion (Patel *et al.* 2004b, Wooding *et al.* 2005). However, no exhaustive analysis has been made of most PAGs in the two phylogenetic groups and taking account the two regions of the placenta. Moreover, the focus of most studies has been at the mRNA level. With the exception of PAG1, the problems encountered in trying to purify the different PAGs from placental extracts without cross-contamination have not enabled the generation of strictly specific antibodies (Butler *et al.* 1982, Xie *et al.* 1991, Wooding *et al.* 2005).

The aim of this study was therefore to exhaustively characterize bovine PAG expression in both the villous areas of cotyledons and the intercotyledonary chorion, at both the mRNA and protein levels. In an attempt to produce convincing and reliable results, we developed specific tools such as RT-PCR primers and antibodies. Immunohistochemistry analyses were also performed in order to determine the regional and cellular expression of PAG proteins. We investigated the expression and localization patterns of PAG in placental tissues from day 60 of gestation (when secondary and tertiary villi are established) resulting in a differentiated and visible cotyledon.

Materials and methods

Animals and sample collection

All procedures relating to the care and use of animals were carried out in accordance with the International Guiding Principles for Biomedical Research Involving Animals, as promulgated by the Society for the Study of Reproduction, and with the European Convention on Animals approved by the French Ministry of Agriculture under French regulations (86/609/EEC, updated on 04/19/1988). The experiments were approved by the local ethics committee (Comethea registration numbers: 12/082 for cows and 12/061 for rabbits). The cows were housed at the Union Nationale des Coopératives d'Élevage et d'Insémination Animale (UNCEIA) experimental facilities (Chateauvillain, France). Oestrus cycles were synchronized using the Crestar method on Holstein breed cows, and artificial insemination was performed as described previously (Constant *et al.* 2011). Six to eight cows per stage of gestation were killed at a local slaughterhouse. The cotyledons and intercotyledonary chorion were collected at 60, 80, 100 or 220 days post insemination (dpi). One half of the tissue was snap frozen in liquid nitrogen and stored at -80°C until analysis and the other half was fixed for immunochemistry analyses.

Design and validation of gene-specific PCR primers

Transcript sequences for bovine PAG were retrieved with the ENTREZ Nucleotide using the Reference Sequence database from GENBANK (<http://www.ncbi.nlm.nih.gov/nucleotide/>). When RefSeq data were not available (PAG3, PAG13 and PAG14), we used predicted mRNA sequences. Pseudogenes were excluded from this study. As previously shown (Telugu *et al.* 2009), we determined that PAG22 (AY911498) was PAG2 (NM_176614). Transcript-specific PCR primer couples were designed using the eprimer3 program of EMBOSS 6.3.1 software using the 'Primer3 mispriming library' section (Rice *et al.* 2000). We included in this library all PAG nucleotide sequences for which we wanted to exclude the non-specific crossing of primers. Primer specificity was verified by sequencing the amplicon produced after the amplification of cDNA from extra-embryonic tissues collected at 60 and 100 dpi. The PCR cycling conditions were as follows: single denaturation step at 94°C for 60 s, then DNA denaturation step at 94°C for 30 s, primer annealing step at 60°C for 30 s and a polymerase extension step at 72°C for 30 s. PCR was performed on a BIOMETRA apparatus for 35 cycles. A final elongation step was performed at 72°C for 15 min. Amplicons were purified and cloned into pGEM-T Easy vector (Promega) in subcloning DH5 α competent cells (Invitrogen). Purified PCR fragments were sequenced by Beckman Coulter Genomics (Takeley, Essex, UK) and their identity was investigated in GENBANK using the NCBI Basic Local Alignment Search Tool (<http://blast.ncbi.nlm.nih.gov/>) for nucleic acid sequences. PCR primer couples corresponding with authenticated fragments were validated and used for the amplification experiments (see Table 1).

Evaluation of PAG gene expression between 60 and 220 dpi

Total RNA was extracted from tissues using the phenol-based method described by Chomczynski & Sacchi (1987). The

Table 1 Sequence of primers for real-time quantitative PCR.

Gene name	Accession number	Oligonucleotide primer sequence 5'-3'		Product size (bp)
		Forward	Reverse	
PAG1	M73962	GGTACCCCTGATCCAAGC	TATGGCACCGATGAGCCTAT	172
PAG2	L06151	GTATCCTGGGCTTGGCTTTT	CCCTCTGGCTTGTGTTGTGTT	183
PAG3 variant 1	XM_002699276	GGGCAGAGCTTATTATGATGG	TCTTGGGCCTTCTATTGCTG	340
PAG4	AF020506	CCACCAAGGTGTGAATGCTT	CAGGCTTCTGTCCATGTGATT	202
PAG5	AF020507	CAGGCAGGTGAGTGGAGTCT	GGCAGGGATATGACAGCAAA	209
PAG6	AF020508	TGGGTCTCAGTACTTCGTTT	TCAGCACCCGTTAAGTGAAG	412
PAG7 variant 2	AF020509	TCGATCGATTGCAACAGTACA	TTGTGCGCAAACCCATATT	215
PAG8	BC133476	CCTGTGCCCCCTGACTACTA	GTAGCAGCCCCGAATTTATGC	206
PAG10	AF020512	GCCCAAGCTTACATCCAAAG	ATTCTGAAGTAGCCAGCA	192
PAG11	AF020513	AGTGATTGGCTGTGAACACG	CACGAGGCACTGAGTAATCG	206
PAG12	AF020514	CACCAAGTTCGGAGTATGT	GGCAGAAGTTTTGAGCCTTG	130
PAG15	AF192332	ACGGATCTGGGACAATGG	ATACCCCGGTGTCAACAA	426
PAG16	AF192333	ATTCGAGCAGGTGACTG	TGTAGATCTCTCACTCTTTGCTC	333
PAG17	AF192334	CGGCATACCCAAAAGGTCT	ACCGTCAAACCCAACTTCTG	144
PAG19	AF192336	AGAATACGGGCTTGAGCATA	TTTCCCCTGTAATAGCGATG	210
PAG20	AF192337	CCGGGTCATCAAATATCCAA	GACAACAGAGGGCAGAGCAC	128
PAG21	AF192338	TCGAGGATTTGATGTACGTG	TGCCATCATAAGCTCTGTCC	327
ACTB	BC102948	GACTACCTCATGAAGATCCTC	CGGATGTCCACGTCACTTC	320
RPL19	BC102223	CCCCAATGAGACCAATGAAATC	CAGCCCATCTTTGATCAGCTT	73
GAPDH	BC102589	GCTGACGCTCCCATGTTTGT	TCATAAGTCCCTCCACGATGC	151

concentration and purity of RNA samples were determined by spectrophotometry at 260 and 280 nm. To estimate RNA integrity, 2 µg of the extract were separated by 0.8% agarose gel electrophoresis under neutral conditions and stained with ethidium bromide. One microgram of total RNA was reverse transcribed into cDNA using 100 IU of Moloney murine leukaemia virus enzyme and 0.5 µg/µl oligo-dT 12–18 primers (Invitrogen), in a total volume of 20 µl at 37 °C for 1 h. Gene expression analysis was performed using real-time quantitative PCR with the SYBRGreen detection assay. The primer pairs are listed in Table 1. The expression of PAG genes was analysed using previously designed primers. β-Actin (*ACTB*), glyceraldehyde 3-phosphate dehydrogenase (*GAPDH*) and ribosomal protein L19 (*RPL19*) were selected as the bovine reference genes for normalization (Table 1). Each amplified PCR fragment was sequenced to assess the amplification of the correct gene. The calculation of amplification efficiency was based on the generation of standard curves using serial dilutions of known concentrations of cloned target amplicons, thus enabling the determination of copy numbers. Two measurements of each sample were performed as technical replicates. Briefly, 5% of the cDNA was added as the PCR template to 12.5 µl 2× SYBRGreen PCR Master Mix (Applied Biosystems), with 300 nM of each forward and reverse primer in a final volume of 25 µl. PCR was performed on the StepOnePlus Real-Time PCR apparatus (Applied Biosystems) using universal cycling conditions: 95 °C for 10 min, then 40 cycles at 95 °C for 15 s and 60 °C for 1 min, followed by a melting curve verification step. The data were analysed using StepOne Software v2.2.2 (Applied Biosystems).

Peptide design for protein-specific polyclonal antibodies and immunoglobulin purification

The 'Antigenic' program of the EMBOSS 6.3.1 software (Kolaskar & Tongaonkar 1990) was used to identify antigenic determinants (epitopes) from the amino acid sequences of PAG2 (NP_788787) and PAG11 (NP_788796). Epitopes were

selected according to their capacity to generate antibodies. This capacity was calculated in relation to the physicochemical properties of the amino acid residues and their frequencies of occurrence. Identified sequences were compared with the complete peptidic sequences of all other PAGs using the NCBI Basic Local Alignment Search Tool and the EBI ClustalW2 multiple sequence alignment tool (<http://www.ebi.ac.uk/Tools/msa/clustalw2/>) to preserve only specific sequences and prevent any inconvenient crossovers. Epitope sequences were used as templates by Proteogenix (Schiltigheim, France) to synthesized corresponding peptide and keyhole limpet hemocyanin (KLH)-conjugated peptides. The PAG1 protein was purified as previously described (INRA patent n° FR-88 03590 and Camous *et al.* (1988)) with minor modifications. The monitoring of PAG in all steps of the purification process was performed using a RIA previously developed (Mialon *et al.* 1993). Briefly, day 150–200 bovine placental cotyledons were homogenized in 0.05 M phosphate buffer at pH 8.6 containing 0.1 M KCl and 20 µM phenylmethanesulfonyl fluoride at 4 °C, using an Ultra-Turrax homogenizer. The total protein extract was acid precipitated at pH 4.3. After centrifugation, the supernatant was fractionated by precipitation with ammonium sulphate at pH 5.2. The 40–65% saturated ammonium sulphate fraction was extensively dialysed against 0.05 M Tris/HCl buffer at pH 8.6. The protein preparation was chromatographed onto a DEAE Sephadex A50 (GE Healthcare Life Sciences, Velizy-Villacoublay, France) column and the protein fractions were eluted by increasing ionic strength using a stepwise gradient of KCl in 0.05 M Tris/HCl buffer at pH 8.6. The 0.3 M KCl fraction was dialysed and concentrated by ultrafiltration and then submitted to cation exchange HPLC chromatography using a TSK-SP 5PW column (21.5×150 mm; Tosoh Bioscience GmbH, Stuttgart, Germany). Proteins were eluted at a flow rate of 4 ml/min by a linear gradient of KCl in the Tris buffer and the protein elution was monitored by u.v. at 280 nm. Finally, the PAG1/PSP60-positive fractions were collected and concentrated by ultrafiltration and next chromatographed onto

a size exclusion TSK-G3000 PW column (7.8×600 mm; Tosoh Bioscience GmbH). These chromatographic processes enabled the purification of a single PAG1/PSP60 protein eluting as a discrete peak. The protein appeared at a unique band around 65 kDa in SDS-PAGE. The N-terminal protein sequence of the first 40 residues (NGSNLTTHPLRNKDLVYMGNITIGTPP-QEFQVVFDTASS-) identified this protein originally called PSP-60 in our laboratory (Camous *et al.* 1988, Mialon *et al.* 1993) at the referred polypeptide chain of bovine PAG1 (UniProtKB accession number: Q29432; Genbank accession number: AAB35845). PAG2 peptides, PAG11 peptides and native PAG1 protein were used to raise anti-PAG2, anti-PAG11 and anti-PAG1 polyclonal antibodies. Antibodies were generated using two New Zealand White rabbits per antigen. The rabbits were primed with an intradermal injection of 80 µg PAG1 or 80 µg KLH-conjugated peptide emulsified in complete Freund's adjuvant (Sigma-Aldrich), followed by several booster immunizations at 3-week intervals with 40 µg protein or KLH-conjugated peptides in incomplete Freund's adjuvant (Sigma-Aldrich). Blood samples were collected 10 days after each injection, starting from the second month after the first antigen injection. Immune sera were separated from whole blood samples after centrifugation for 30 min at 3500 *g* and at 4 °C and then stored at -20 °C. Immunoglobulins were purified from anti-PAG1 (L520), anti-PAG2 (L390) and anti-PAG11 (L349) immune sera by affinity chromatography onto an Hitrap NHS-activated HP pre-packed column (GE Healthcare). The protein or peptides were first immobilized on the column according to the manufacturer's instructions. The columns were equilibrated with 20 mM phosphate buffer at pH 7.1. Immunoglobulins were eluted with 0.2 M glycine/HCl at pH 2.8 and then dialysed and concentrated against a neutral phosphate buffer using an Amicon ultrafiltration unit with a YM10 membrane (Millipore, Guyancourt, France).

Western blot analysis

Placental proteins were extracted from small pieces of tissue by sonication in a cold lysis buffer at pH 7.4 containing 50 mM HEPES, 150 mM NaCl, 5 mM EDTA, 16 mM 3-[(3-cholamidopropyl) dimethylammonio]-2-hydroxy-1-propanesulfonate, 1 mM benzimidazole HCl, 1 mM phenylmethylsulfonyl fluoride, 10 µg/ml soybean trypsin inhibitor, 10 µg/ml leupeptin and 10 µg/ml aprotinin. Protein quantification was performed with the Bio-Rad protein assay (Bio-Rad) using BSA as the standard (Sigma-Aldrich). Twenty micrograms of each sample were separated by 10% SDS-PAGE and electro-transferred onto a Hybond-P PVDF membrane (GE Healthcare). Protein molecular weight markers (ProSieve Color Protein Markers, Lonza, Levallois-Perret, France) and samples were run simultaneously. After washing in Tris-buffered saline containing Tween 20 (TBST) (50 mM Tris at pH 7.5, 137 mM NaCl and 0.1% Tween 20), the membranes were blocked in 2% TBST BSA and 0.2% Tween 20 overnight at 4 °C. Dedicated blots were probed for 2 h at room temperature with immunoglobulin anti-PAG1, anti-PAG11 and anti-PAG2 diluted in 2% TBST BSA 0.2% Tween 20 used at a final concentration of 0.5, 0.4 and 1.7 µg/ml respectively. Peroxidase-conjugated donkey anti-rabbit IgG (Jackson ImmunoResearch, Interchim,

Montluçon, France) was used as the secondary antibody, diluted to 1:20 000 (vol/vol) and incubated for 1 h 30 min at room temperature. Two negative control experiments were also performed: in the first case the primary antibodies were omitted and in the second the primary antibody was neutralized with the peptide or protein used as the immunogen. Antibodies were pre-incubated for 30 min at 38 °C with 10 µg of the respective protein or peptide per microgram of immunoglobulin. To control for variations in extraction and loading, each blot was probed with rabbit polyclonal anti-GAPDH (diluted 1:1000; Santa Cruz) after stripping the membranes for 30 min at 56 °C in 50 mM Tris/HCl, 2% SDS and 100 mM β-mercaptoethanol. The antibodies were examined for cross-reactions in slot blot assays. Proteins and peptides were diluted in 50 mM Tris/HCl at pH 7.5 containing 0.005% bromophenol blue. Different loading volumes were used to increase the quantity range of the peptides and protein. Samples were blotted onto a PDVF membrane using a Manifold II SRC 072/00 blotter (Schleicher & Schuell, Dassel, Germany). The membranes were probed as for western blot. Immunoreactive signals were revealed with the Pierce western blot signal enhancer reagent system (Thermo-fisher, Illkirch, France) and chemiluminescence was visualized using a CCD camera (LAS1000, Fujifilm, Düsseldorf, Germany). The data were analysed with Advanced Image Data Analyser Software (Raytest, La Defense, France).

Enzymatic N-deglycosylation

Protein extracts from the cotyledon and intercotyledonary chorion harvested at 220 dpi were subjected to enzymatic digestion to remove oligosaccharides using peptide *N*-glycosidase F (New England Biolabs, Evry, France) according to the supplier's instructions. Briefly, 20 µg of the total protein extract were denatured for 10 min at 100 °C in glycoprotein-denaturing buffer at a final volume of 10 µl. After cooling, the samples were treated with 100 IU PNGase-F for 2, 5, 15, 30, 90 and 360 min at 37 °C. Mock-treated protein extracts were incubated without the enzyme as controls. The reaction was terminated by PNGase-F inactivation under incubation at 75 °C for 10 min. The samples were then frozen in liquid nitrogen until western blot analysis as described earlier.

Immunohistochemical investigations

After 4-h fixation in 4% paraformaldehyde in 0.1 M phosphate buffer, pH 7.5, at 4 °C and a wash in the same buffer, all samples were embedded in paraffin (Paraplast plus, Sigma-Aldrich) in an automated system (Shandon Citadel Tissue Processor; Thermo-fisher) and stored at 4 °C. Sections of tissue were cut at microtome settings of 5 or 8 µm with an RM2245 apparatus (Leica Microsystems SAS) and recovered on Super Frost Plus slides (Thermo-fisher). The tissue sections were deparaffinized in xylene and rehydrated stepwise in ethanol (100, 95, 70 and 30%) followed by a final rehydration in 0.1 M phosphate buffer at pH 7.5. Individual sections were enclosed in a hydrophobic barrier using an ImmEdge pen (Vector Laboratories, Clinisciences, Nanterre, France) and treated successively for antigen unmasking in 0.01 M trisodium citrate at pH 6.0 for 5 min at room temperature and then 10 min at 80 °C. To quench

endogenous peroxidase activity, the slides were treated for 30 min with 0.1% hydrogen peroxide (by volume). The primary antibody was used as a purified immunoglobulin at 0.05, 0.4 and 1.7 µg/ml for PAG1, PAG11 and PAG2 respectively. Antibodies were diluted in 0.1 M phosphate buffer at pH 7.5 containing 2% BSA (wt/vol) and donkey serum diluted 1:100 (vol/vol). The slides were incubated overnight at 4 °C with the primary antibody. After two washes in 0.1 M phosphate buffer at pH 7.5 containing 0.2% BSA, the slides were incubated for 1 h at room temperature with the secondary biotinylated donkey anti-rabbit antibody (Jackson ImmunoResearch) diluted 1:1000 (vol/vol) in 0.1 M phosphate buffer at pH 7.5 with 2% BSA. As for western blotting, two negative control experiments were carried out. The primary antibody was either omitted or immunoneutralized by an excess of the protein or peptide. The slides were then incubated for 1 h with Vectastain Elite ABC-HRP reagent (Vector Laboratories) in 50 mM Tris/HCl buffer at pH 7.6 to activate the avidin–biotin peroxidase complex. After washing in the same buffer, the peroxidase was visualized with nickel-enhanced diaminobenzidine tetrahydrochloride chromogen (5 mg/ml ammonium nickel (II) sulphate; 0.5 mg/ml diaminobenzidine tetrahydrochloride). Incubation was performed at 25 °C for 5 min to achieve purple staining. Finally, the sections were fixed in 2% paraformaldehyde for 5 min and gradually dehydrated in successive baths of 90% ethanol, 100% ethanol, 50% ethanol–50% Neo-Clear (vol/vol) (Merck) and 100% Neo-Clear. The tissue sections were mounted using permanent Neo-Mount medium (Merck).

The simultaneous immunodetection of PAG1 and PAG11 on the one hand and of PAG1 and PAG2 on the other hand was performed using double immunoenzymatic labelling. PAG2 and PAG11 were first located according to the protocol described earlier. However, to enable compatibility between the chromogens, the bound antibodies were visualized using ImmPACT Novared peroxidase substrate (Vector Laboratories) according to the supplier's instructions. After peroxidase detection, the tissue sections were washed twice for 5 min in 0.1 M phosphate buffer at pH 7.5 containing 0.2% BSA and incubated for 30 min at 38 °C in 0.2 µg/ml alkaline phosphatase-conjugated anti-PAG1 immunoglobulin. The anti-PAG1 immunoglobulin had previously been covalently bonded to alkaline phosphatase using the lightning-link AP conjugation kit (Innova Biosciences, Interchim, Montluçon, France). After two washes in 0.1 M phosphate buffer at pH 7.5, the slides were incubated for 30 min with Vector Blue alkaline phosphatase substrate (Vector Laboratories) in 0.1 M Tris/HCl at pH 8.2 containing 0.1% Tween 20 according to the supplier's instructions. The slides were then rinsed, dehydrated and mounted as described earlier. Photomicroscopies were captured using the NanoZoomer Digital Pathology System and images were visualized with NDPview (NanoZoomer Digital Pathology Virtual Slide Viewer Software, Hamamatsu, Massy, France). The experiments were repeated on three different placental sections from two 220 dpi cows.

Statistical analyses

Quantitative results were analysed using SYSTAT software v11 (Systat Software, Inc., Erkrath, Germany). The data were subjected to two-way ANOVA with the day of gestation and

the type of placental tissues (cotyledonary and intercotyledonary chorion) as the main categories and day-by-tissue interactions. If a day-by-tissue interaction was evidenced, one-way ANOVA was performed and followed by pairwise comparisons using the Bonferroni adjustment. Data are expressed as least squares means \pm S.E.M.

Results

Design and validation of gene-specific PCR primers

Specific amplification primers were successfully designed for 16 of the 21 PAGs. PCR was thus performed on extra-embryonic tissues at two stages of gestation (days 60 and 100) with amplification of a single fragment. A BLAST search indicated 100% identity of the generated amplicons with the targeted PAGs.

Expression of PAG genes in the cotyledon and intercotyledonary chorion during gestation

ANOVA indicated that PAG mRNAs could be assigned to three different sets as a function of their distribution between different placental zones (Figs 1, 2 and 3). The first set included *PAG1*, *PAG2*, *PAG3*, *PAG15*, *PAG17* and *PAG21*, which were twice to four times more expressed in the cotyledonary tissue than in the intercotyledonary chorion ($P < 0.001$) where they remained at low levels (Fig. 1). For all these genes, two-way ANOVA highlighted an interaction between tissue distribution and the day of gestation ($P < 0.001$). This illustrated a marked increase in gene expression in the cotyledon as a function of the day of gestation but few changes in the intercotyledonary chorion. One-way ANOVA indicated that *PAG1* was increasingly expressed in the cotyledon ($P < 0.001$). Pairwise comparisons revealed that *PAG1*, which was at its lowest levels on day 60, increased significantly from days 60 to 80 ($P < 0.001$), remained at steady-state levels between days 80 and 100 ($P < 0.01$) and was expressed at its highest levels on day 220 ($P < 0.001$). In the intercotyledonary chorion, *PAG1* slightly increased during gestation ($P < 0.01$) with the most significant difference between days 60 and 100 ($P < 0.05$). In the cotyledon, *PAG2*, which was at its lowest levels on day 60, increased significantly from days 60 to 80 ($P < 0.001$), decreased by day 100 ($P < 0.01$) and became expressed at its highest levels by day 220 ($P < 0.001$). In the intercotyledonary chorion, the expression of *PAG2* progressively decreased ($P < 0.01$) with the most significant difference between days 60 and 220 ($P < 0.001$). In the cotyledon, *PAG3* exhibited a similar profile to *PAG1*, with the highest levels of expression on day 220 compared with day 60 ($P < 0.001$), day 80 ($P < 0.001$) and day 100 ($P < 0.001$). No difference was observed between days 80 and 100 of gestation. In the intercotyledonary chorion, *PAG3* was expressed at low levels on day 80 compared with day 220 ($P < 0.01$). In the

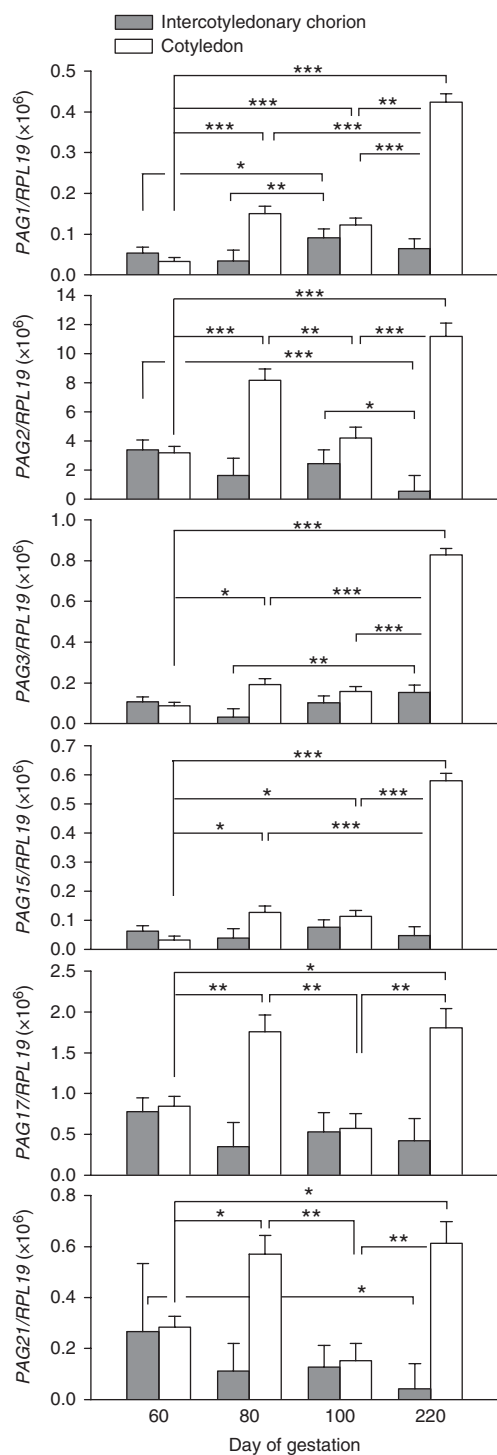


Figure 1 Expression of modern *PAG1*, *PAG3*, *PAG15*, *PAG17* and *PAG21* and ancient *PAG2* in the placental chorion from 60 to 220 dpi. This group represents PAGs that are mainly expressed in the cotyledon ($P < 0.001$ for *PAG1*, *PAG2*, *PAG3*, *PAG15*, *PAG17* and *PAG21*). Intercotyledonary and cotyledonary chorion specimens were collected from pregnant cows at 60, 80, 100 and 220 dpi (cows = 6–8 per stage). PAG mRNAs were quantified by RT-qPCR and the results were normalized to *RPL19*. Data are presented as mean \pm S.E.M. Pairwise tests of mean differences were performed after significant one-way ANOVA: * $P < 0.05$; ** $P < 0.01$; *** $P < 0.001$.

cotyledon, *PAG15* displayed similar gene expression profile to *PAG1* and *PAG3*. *PAG15* was at its highest levels on day 220 compared with day 60 ($P < 0.001$), day 80 ($P < 0.05$) and day 100 ($P < 0.05$). The levels of expression were similar between days 80 and 100 ($P > 0.05$). No differences in *PAG15* expression levels were observed in the intercotyledonary chorion. In the cotyledon, *PAG17* and *PAG21* showed similar patterns of expression to *PAG2* with two maxima on days 80 and 220 and two minima on days 60 and 100. *PAG17* and *PAG21* were twofold more abundant on days 80 and 220 than on days 60 and 100 ($P < 0.01$). In the intercotyledonary chorion, no changes in *PAG17* expression were observed throughout the gestation whereas *PAG21* was expressed at lower levels on day 220 compared with day 60 ($P < 0.05$). The second set comprised *PAG8*, *PAG10*, *PAG11* and *PAG12* (Fig. 2). These PAGs were strongly expressed in the intercotyledonary chorion between days 60 and 220 of gestation whereas they only displayed weak expression in the cotyledon ($P < 0.001$). *PAG8*, *PAG10*, *PAG11* and *PAG12* were respectively 5-, 21-, 26- and 4-fold, respectively, more strongly expressed in the intercotyledonary chorion than in the cotyledon. According to the mRNA copy numbers, *PAG8* was the most strongly expressed transcript in this second set. *PAG8*, *PAG10* and *PAG11* were significantly affected by a day-by-placental zone interaction ($P < 0.001$). In the intercotyledonary chorion, *PAG8*, *PAG10* and *PAG11* regularly increased during the gestation ($P < 0.001$) (Fig. 2). However, the increase in gene expression was more significantly pronounced in late gestation than in early and middle gestation (day 220 vs day 60: *PAG8* ($P < 0.001$), *PAG10* ($P < 0.001$) and *PAG11* ($P < 0.001$)). *PAG8* remained nearly unchanged until day 220. *PAG10* was significantly augmented on day 100 (day 60 vs day 100: $P < 0.05$) and reached maximum levels on day 220 (day 60 vs day 220: $P < 0.001$). The level of *PAG11* increased gradually from days 60 to 100 and was intensively up-regulated on day 220 (day 60/day 80/day 100 vs day 220: $P < 0.001$). *PAG12* was expressed at constant levels in the two placental zones whatever the day of gestation. In the cotyledon, *PAG8* and *PAG11* were expressed at constant and low levels while *PAG10* exhibited a small increase on day 220 compared with the other periods of gestation ($P < 0.001$). The third set contained *PAG7* and *PAG16*, which were not differentially expressed between the cotyledon and intercotyledonary chorion ($P > 0.05$) (Fig. 3). In the cotyledon, *PAG7* was expressed at similar levels throughout the period of gestation studied. In the intercotyledonary chorion, *PAG7* was at its lowest level on day 80 and this was significantly different to that on day 60 ($P < 0.01$). *PAG16* was differentially expressed between days of gestation in both placental zones. In the cotyledon, *PAG16* expression was higher on day 220 compared with day 100 ($P < 0.05$) and day 60 ($P < 0.01$). In the intercotyledonary chorion, *PAG16* expression differed between days 80 and 100

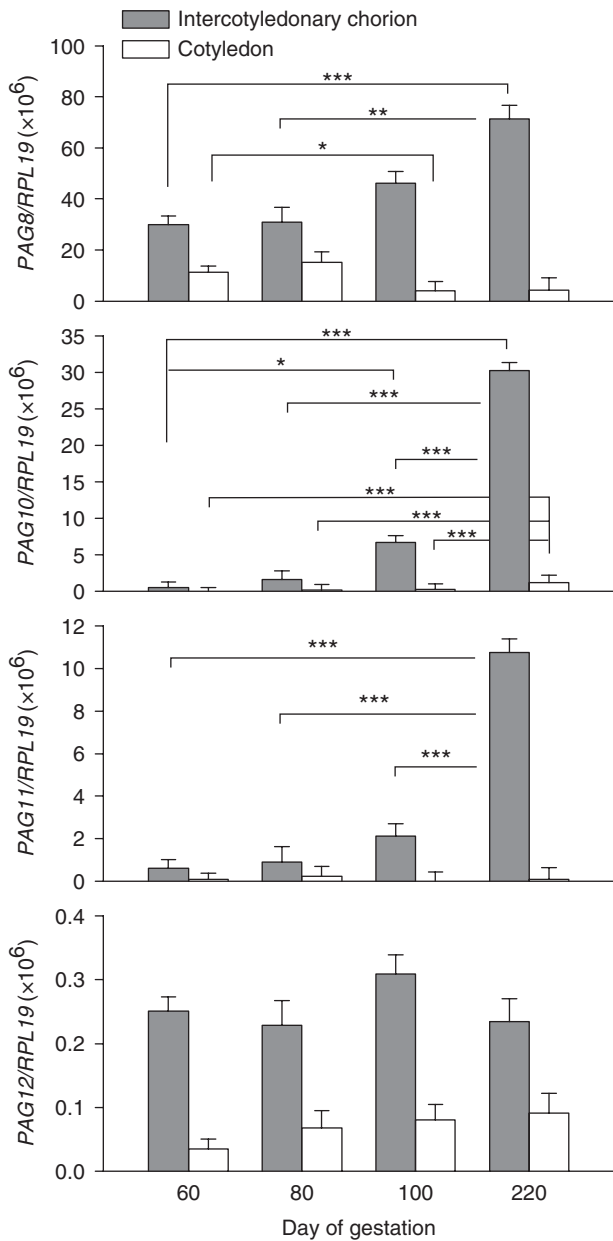


Figure 2 Expression of ancient *PAG8*, *PAG10*, *PAG11* and *PAG12* in the placental chorion from 60 to 220 dpi. This group represents PAGs that are mainly expressed in the intercotyledonary chorion ($P < 0.001$ for *PAG8*, *PAG10*, *PAG11* and *PAG12*). Intercotyledonary and cotyledonary chorion specimens were collected from pregnant cows at 60, 80, 100 and 220 dpi (cows = 6–8 per stage). PAG mRNAs were quantified by RT-qPCR and the results were normalized to *RPL19*. Data are presented as mean \pm S.E.M. Pairwise tests of mean differences were performed after significant one-way ANOVA: * $P < 0.05$; ** $P < 0.01$; *** $P < 0.001$.

($P < 0.01$). Finally, the levels of expression of four other PAG (*PAG4*, *PAG5*, *PAG6* and *PAG19*) were determined. Because they were expressed at low levels close to the limit of detection of real-time PCR, and because they displayed no significant variations, the data on them are not shown. We observed that set-1 comprised modern

PAGs whereas set-2 (characterized by expression in the intercotyledonary chorion) contained exclusively ancient PAGs. However, *PAG2*, which was expressed in the cotyledon but not in the intercotyledonary chorion, belonged to the ancient group.

PAG expression in the cotyledon and intercotyledonary chorion during gestation

The partitioning of PAG between the cotyledon and intercotyledonary chorion as evidenced by the study of mRNA was also examined at the protein level. This investigation was performed on three PAGs, two of which were representative of the two main patterns revealed by the mRNA study (sets 1 and 2). *PAG1* was selected as the archetype of PAGs primarily expressed by the cotyledon (set 1), while *PAG11* was considered to be typical of PAGs predominantly expressed in the intercotyledonary chorion of the placenta. Finally, we investigated the *PAG2* protein that emerged as an atypical PAG representative of the ancient group.

Characterization of antibodies

Antibodies were purified as IgG using affinity chromatography with the natural protein *PAG1* or peptides as ligands. The antibodies were characterized using protein

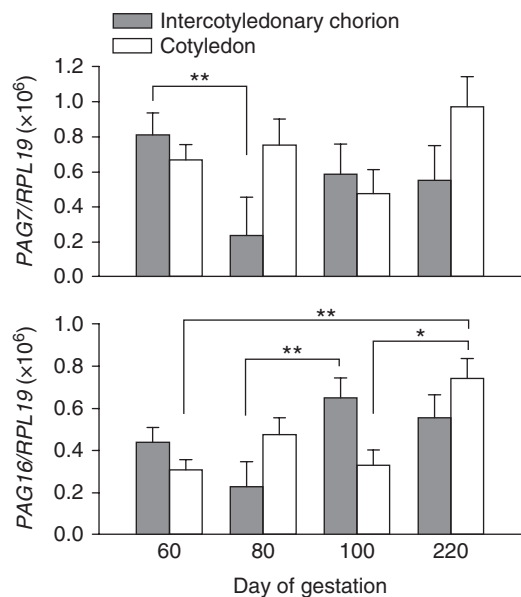


Figure 3 Expression of modern *PAG7* and *PAG16* in the placental chorion from 60 to 220 dpi. This group represents PAGs that are expressed at equivalent levels in the cotyledonary and intercotyledonary chorion ($P > 0.05$ for *PAG7* and *PAG16*). Intercotyledonary and cotyledonary chorion specimens were collected from pregnant cows at 60, 80, 100 and 220 dpi (cows = 6–8 per stage). PAG mRNAs were quantified by RT-qPCR and the results were normalized to *RPL19*. Data are presented as mean \pm S.E.M. Pairwise tests of mean differences were performed after significant one-way ANOVA: * $P < 0.05$; ** $P < 0.01$.

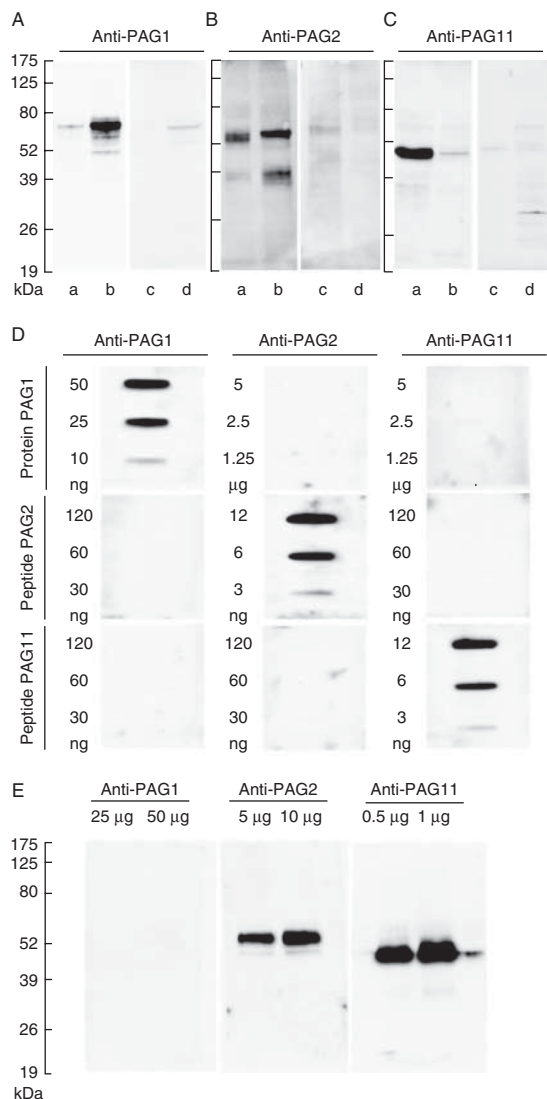


Figure 4 Validation of antibodies. (A, B and C) Western blot of PAG1, PAG2 and PAG11 in the bovine intercotyledonary and cotyledonary chorion at 220 days of gestation. Membranes were incubated in the presence of anti-PAG1 (L520) (A), anti-PAG2 (L390) (B) and anti-PAG11 (L349) (C) immunoglobulins in the intercotyledonary (a and c) and cotyledonary (b and d) chorion. Immunoneutralization was performed and involved the pre-incubation of antibodies in the presence of antigens (c and d). The antibodies revealed major bands at 67, 53 and 44 kDa for PAG1, PAG2 and PAG11 respectively. (D) Slot blot of anti-PAG1, anti-PAG2 and anti-PAG11 against the purified PAG1 protein and PAG2 and PAG11 synthetic peptides. To evaluate cross-reactivities, the protein and peptides were fixed in increasing quantities on membranes and incubated in the presence of anti-PAG1 (L520), anti-PAG2 (L390) or anti-PAG11 (L349). The anti-PAG1 revealed an immunoreactive signal only against the PAG1 protein, the anti-PAG2 only against the PAG2 peptide and the anti-PAG11 only against the PAG11 peptide. (E) Western blot of PAG1, PAG2 and PAG11 in day 16 bovine conceptuses. Increasing quantities of protein extracts were transferred onto membranes and incubated in the presence of anti-PAG1 (L520), anti-PAG2 (L390) and anti-PAG11 (L349) immunoglobulins. The anti-PAG1 did not reveal any signal in the day 16 conceptuses, and the anti-PAG2 and anti-PAG11 revealed dose-related immunoreactive signals at 53 and 44 kDa respectively.

extracts from the cotyledon and intercotyledonary chorion at days 100 and 220. Only, data from day 220 were shown. Figure 4A, B and C shows the western blot results for PAG1, PAG2 and PAG11 respectively. The anti-PAG1 antibody (L520) revealed a major band at 67 kDa (Fig. 4A lanes a and b) that was suppressed when the purified native protein was used to immunoneutralize the antibody (Fig. 4A lanes c and d). The anti-PAG2 antibody (L390) displayed a main band at 53 kDa and a minor immunoreactive protein at 33 kDa (Fig. 4B, lanes a and b). These two signals were suppressed when the PAG2 antigenic peptide was used to immunoneutralize the immunoglobulin (Fig. 4B, lanes c and d). The PAG2 signal at 53 kDa was eight times stronger than the 33 kDa immunoreactive signal. PAG11 was evidenced as a unique protein band at 44 kDa (Fig. 4C lanes a and b) with the anti-PAG11 (L349). Immunoneutralization of the antibody with the peptide resulted in disappearance of the protein signal (Fig. 4C lanes c and d). The antibodies were examined for their cross-reactions in slot blot assays (Fig. 4D). The anti-PAG2 and anti-PAG11 antibodies did not recognize the purified PAG1 protein whereas they produced intensive signals against their respective antigenic peptide. The anti-PAG2 antibody did not display cross-reactivity with the PAG11 peptide even in the presence of significant amounts of the peptide. Similarly, the anti-PAG11 antibody did not cross-react with the PAG2 peptide. The anti-PAG1 antibody failed to recognize both the PAG2 peptide and the PAG11 peptide. An additional validation of the specificity of antibodies was performed using western blot of protein extracts from day 16 bovine conceptuses (Fig. 4E). Until day 25 of gestation, bovine conceptuses were known to not express PAG1 whereas they expressed PAG2 and PAG11 (Green *et al.* 2000). The fact that the anti-PAG1 antibody did not reveal any protein in the conceptus extract while anti-PAG2 and anti-PAG11 showed strong signal indicates that the anti-PAG1 did not cross-react with PAG2 and PAG11 proteins. In the same protein extract, the anti-PAG2 and anti-PAG11 antibodies revealed proteins at different molecular masses, corresponding to the molecular masses recorded in Fig. 4B and C. Taken together, these different lines of evidence, in addition to results from deglycosylation experiments (see below), validate the specificity of the three antibodies used and the lack of cross-reactivity.

Enzymatic N-deglycosylation of PAG1, PAG2 and PAG11 using PNGase-F

Previous results obtained using SDS-PAGE had indicated apparent molecular masses of 67, 53 and 44 kDa for PAG1, PAG2 and PAG11 respectively. The expected molecular mass of PAG polypeptides was around 37 kDa. PAGs are glycoproteins that are predicted to have up to six putative N-glycosylation sites (Xie *et al.*

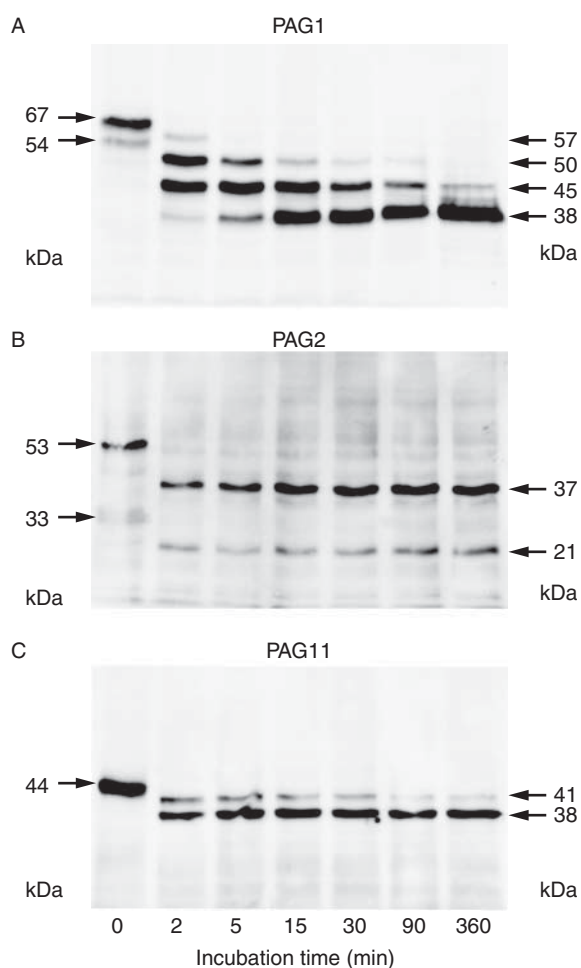


Figure 5 Enzymatic *N*-deglycosylation using PNGase-F. Western blot revealed the enzymatic *N*-deglycosylation of PAG1 (A), PAG2 (B) and PAG11 (C). Proteins were extracted from the cotyledonary (A and B) and intercotyledonary (C) chorion at 220 dpi. Enzymatic *N*-deglycosylation was performed using PNGase-F for 0, 2, 5, 15, 30, 90 and 360 min. During incubation, successive deglycosylation steps yielded 57, 50, 45 and 38 kDa bands from the native 67 kDa PAG1. Fully glycosylated PAG2 at 53 kDa shifted to 37 kDa after deglycosylation. A minor anti-PAG2 immunoreactive band at 33 kDa shifted to 21 kDa. Native PAG11 at 44 kDa produced two deglycosylated proteins at 41 and 38 kDa after the PNGase-F treatment.

1991, 1995, 1997, Klisch *et al.* 2005). We decided to reinforce the capacity of the antibodies generated in order to identify the different PAGs by examining the protein during an enzymatic deglycosylation process. PNGase-F was used to eliminate sugar residues at the *N*-amino glycosylation sites of the amino acid structure. To determine the number of glycosylation sites, PNGase-F was incubated for between 2 min and 3 h (Fig. 5). As depicted on the western blot, enzymatic digestion indicated five protein bands for PAG1 (Fig. 5A). The protein with the highest molecular mass was the native protein. The band for the smallest molecular mass (37 kDa) corresponded to the entirely deglycosylated PAG1. Three bands were interposed between the

native protein and the deglycosylated polypeptide, indicating four *N*-glycosylation sites for PAG1. Digestion of the immunoreactive PAG2 protein generated one band at 37 kDa (Fig. 5B), indicating that PAG2 displayed only one *N*-glycosylation site. A minor immunoreactive protein detected at 33 kDa shifted to 21 kDa, indicating that this protein was also *N*-glycosylated. Both glycosylated and deglycosylated forms of this protein were smaller than the expected size of the PAG2 polypeptide. We suggest that this protein is a truncated PAG2 resulting from proteolytic processing that might occur *in vivo*. The progressive deglycosylation of PAG11 resolved only one band at the polypeptide size (38 kDa), suggesting only two *N*-glycosylation sites (Fig. 5C). Based on the shifts observed in western blot, glycan residues differed in size for the three PAGs examined: 6, 17 and 3 kDa for PAG1, PAG2 and PAG11 respectively.

PAG profiles during gestation

The antibodies thus characterized were then used to examine the expression of PAGs in cotyledonary and intercotyledonary regions in 60- to 220-day-old bovine placentas. Figures 6, 7 and 8 show typical western blot profiles and protein quantifications for PAG1, PAG2 and PAG11 respectively. The experiments were conducted four times on four different cows. Quantitative analysis of signal indicated that PAG1 was four times more concentrated in the cotyledon than in the intercotyledonary chorion ($P < 0.001$) (Fig. 6). A significant interaction was detected between day of gestation and placental zones ($P < 0.01$). This reflected the concomitant trend towards an increase in the amount of PAG1 in the cotyledon and a decrease in the amount of PAG1 in the intercotyledonary chorion. In the cotyledon, PAG1 was at a low concentration at day 60 and reached a maximum as soon as day 80 (day 60 vs day 80: $P < 0.01$; day 60 vs day 220: $P < 0.001$). In the intercotyledonary chorion, a progressive threefold decrease from days 60 to 220 was observed for PAG1 ($P < 0.01$). Similar to PAG1, PAG2 was mainly detected in the cotyledons (Fig. 7). The protein was four times more concentrated in the cotyledon than in the intercotyledonary chorion ($P < 0.001$). The quantities of PAG2 in the intercotyledonary chorion displayed a twofold decrease as gestation progressed, detectable as soon as day 80 (day 60 vs day 80: $P < 0.001$). The concentration of protein remained unchanged in cotyledons ($P > 0.05$). Contrary to PAG1 and PAG2, PAG11 was mostly detected in the intercotyledonary chorion (Fig. 8). The protein was four times more concentrated in the intercotyledonary chorion than in the cotyledon ($P < 0.001$). In the intercotyledonary chorion, PAG11 was consistently expressed at day 60 of gestation and remained at similar levels at days 80 and 100. The concentration of the protein increased to reach its maximum levels at day 220 of gestation (day 60 vs day

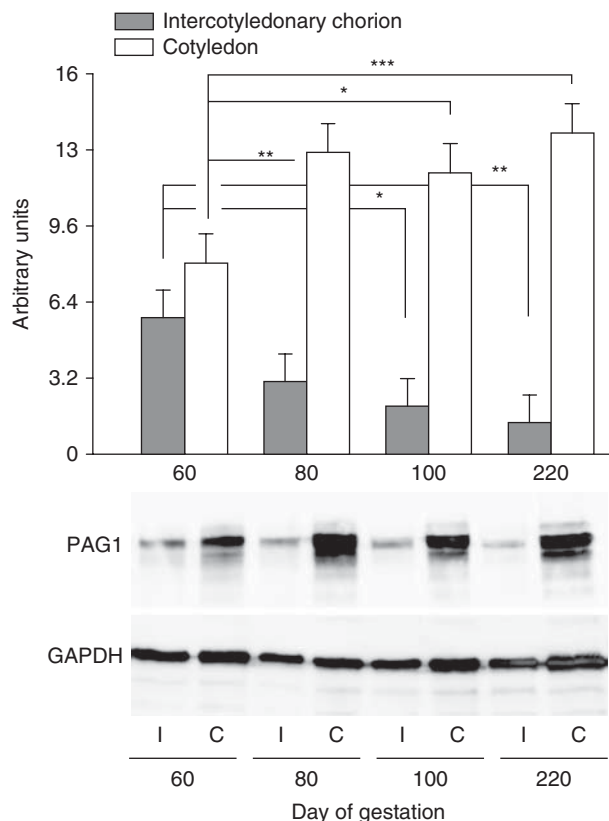


Figure 6 Western blot analyses of PAG1 protein in bovine intercotyledonary (I) and cotyledonary (C) chorion from 60 to 220 days of gestation. The histogram represents the quantification of 67 kDa PAG1 in four independent blots representing four different cows. After PAG detection, the membranes were stripped and probed with anti-GAPDH antibody to confirm the equal loading of samples onto the gel. Two-way ANOVA indicated that PAG1 was more concentrated in cotyledon than in intercotyledonary chorion ($P < 0.001$). Pairwise tests of mean differences were performed if one-way ANOVA showed significance: * $P < 0.05$; ** $P < 0.01$; *** $P < 0.001$.

220: $P < 0.001$). In the cotyledon, no changes in protein concentration were observed during the periods of gestation studied.

Cellular localization of PAG1, PAG2 and PAG11

In order to identify the cellular populations responsible for PAG synthesis, immunohistochemistry was performed on placentomes and intercotyledonary chorion sections at 60, 80, 100 and 220 days of gestation. Only the data relative to day 220 are shown. PAG1 was only detected in the cytoplasm of trophoblastic binucleate cells that were characterized by their round shape and large unstained circular nuclei (Fig. 9B, C and E). PAG1-positive binucleate cells were numerous in placental villi of the whole placentome and in the interplacentomal trophoblastic cell layer (Fig. 9A and D). Mononucleate trophoblastic cells were not stained. Maternal tissues were unmarked.

PAG2 was mainly detected in trophoblastic placental cells (Fig. 10A). Rare cells were weakly labelled in the intercotyledonary regions (Fig. 10D and E). PAG2 staining was concentrated in the trophoblast cell layer surrounding binucleate cells that appeared to be unstained. The anti-PAG2 antibody labelled mononucleate trophoblastic cells that were cuboidal or columnar (Fig. 10C). PAG2-positive mononuclear cells were not equally distributed within the placentome. Mononucleate trophoblastic cells from secondary and tertiary villi were stained (Fig. 10C) whereas no signal was detected in the stem villi and chorionic plate (Fig. 10B).

The anti-PAG11 antibody labelled trophoblastic cells from both the placentome and the intercotyledonary chorion (Fig. 11A and D). In these two regions, PAG11 was only detected in trophoblastic binucleate cells. Mononucleate cells were unstained (Fig. 11B and E). In the placentome, only binucleate cells located at the chorionic plate were labelled (Fig. 11A and B) whereas binucleate cells in the secondary and tertiary villi were unstained (Fig. 11A and C). As for PAG1, numerous

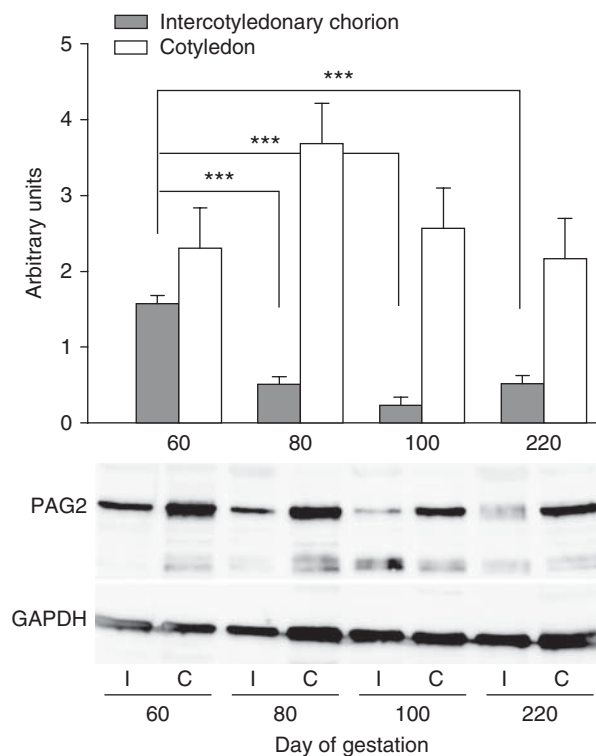


Figure 7 Western blot analyses of PAG2 protein in bovine intercotyledonary (I) and cotyledonary (C) chorion from 60 to 220 days of gestation. The histogram represents the quantification of 53 kDa PAG2 in four independent blots representing four different cows. After PAG detection, the membranes were stripped and probed with anti-GAPDH antibody to confirm the equal loading of samples onto the gel. Two-way ANOVA indicated that PAG2 was more concentrated in cotyledon than in intercotyledonary chorion ($P < 0.001$). Pairwise tests of mean differences were performed if one-way ANOVA showed significance: *** $P < 0.001$.

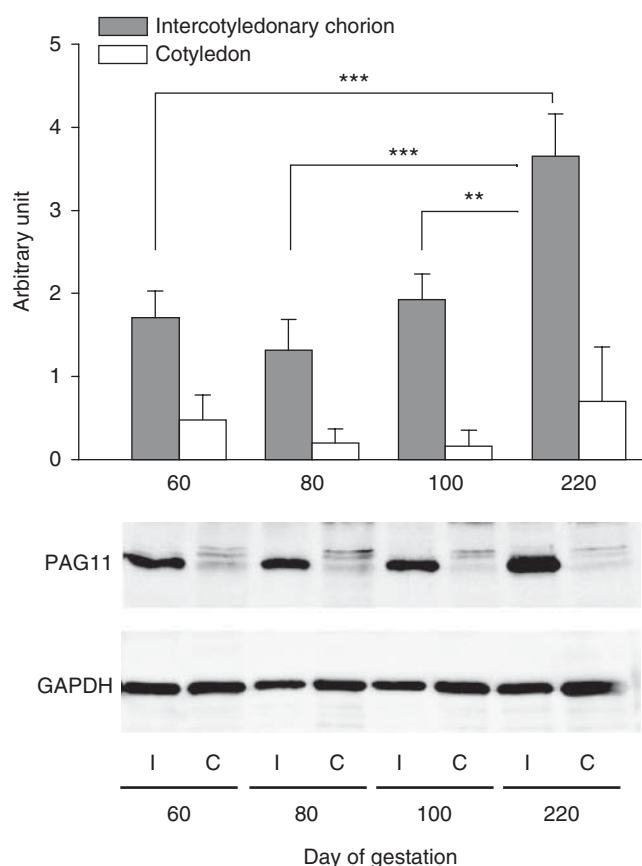


Figure 8 Western blot analyses of PAG11 protein in bovine intercotyledonary (I) and cotyledonary (C) chorion from 60 to 220 days of gestation. The histogram represents the quantification of 44 kDa PAG11 in four independent blots representing four different cows. After PAG detection, the membranes were stripped and probed with anti-GAPDH antibody to confirm the equal loading of samples onto the gel. Two-way ANOVA indicated that PAG11 was more concentrated in intercotyledonary chorion than in cotyledon ($P < 0.001$). Pairwise tests of mean differences were performed after significant one-way ANOVA: ** $P < 0.01$; *** $P < 0.001$.

binucleate cells in the intercotyledonary chorion were PAG11 positive (Fig. 11D and E). PAG11 was also characterized by homogenous cytoplasmic staining and was not detected in mononucleate cells. PAG1, PAG2 and PAG11 staining disappeared after immunoneutralization of the antibody with purified PAG1 protein or the corresponding peptides specific to PAG2 and PAG11 respectively (Figs 9F, 10F and 11F).

In the chorionic plate of the placentome and in the intercotyledonary chorion, both PAG1 and PAG11 were detected in binucleate trophoblastic cells. We tried to determine whether the antibodies targeted the same binucleate cells or whether PAG1 and PAG11 were synthesized by two distinct subpopulations of binucleate cells. Figure 12 shows the localization of PAG11 and PAG1 in the intercotyledonary chorion. PAG11 was revealed by anti-rabbit IgG-peroxidase antibody using NovaRed as the substrate and appears in red. PAG1 was

revealed by anti-PAG IgG conjugated to alkaline phosphatase using VectorBlue as the chromogen substrate and appears in blue. PAG1-positive cells were mainly distributed in clusters and exceptionally as single positive cells throughout the trophoblastic layer of the chorion (Fig. 12A). No binucleate trophoblastic cells were recorded as being simultaneously stained with both PAG1 and PAG11 (Fig. 12B). Double-staining procedures using anti-PAG1 and anti-PAG2 antibodies are shown in Fig. 13. PAG1 was revealed in binucleate cells of the trophoblastic villi (Fig. 13A, B and C). Positive staining for PAG2 was clearly confined to mononucleate trophoblastic cells. No PAG2 staining was observed in binucleate cells expressing PAG1 (Fig. 13B and C).

Discussion

As far as we know, this is the first comparative study to have focused on the expression of ancient and modern PAGs in both the cotyledon and the intercotyledonary chorion of the bovine placenta. The innovative nature and relevance of our investigation were based on the use of advanced analytical tools for both transcript and

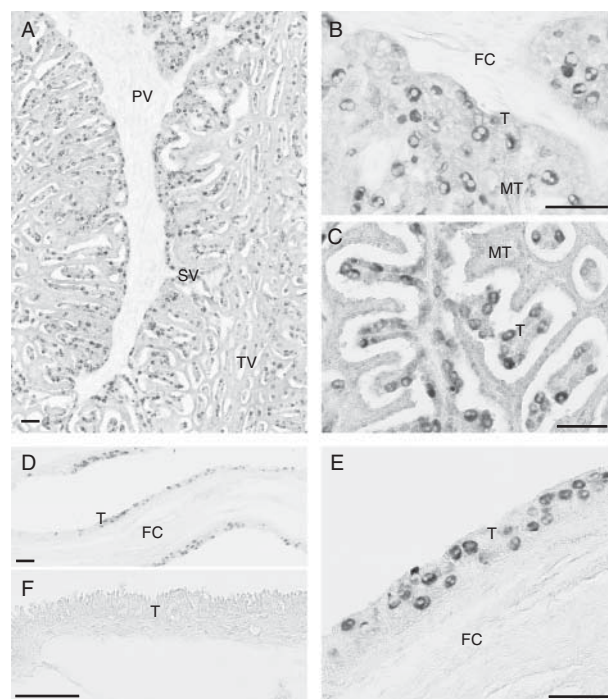


Figure 9 Immunohistochemistry of PAG1 protein in bovine placental (A, B and C) and interplacentomal (D, E and F) tissue sections at 220 days of gestation using the anti-PAG1 (L520) antibody. Panel A illustrates a global section of the placentome. Panel B illustrates the chorionic plate of the placentome. Panel C illustrates the internal secondary and tertiary villi. Panel F shows immunoneutralization of the anti-PAG1 antibody with the PAG1 protein. The anti-PAG1 antibody labelled only binucleate cells. PV, primary villi; SV, secondary villi; TV, tertiary villi; FC, foetal connective tissue; MT, maternal tissue; T, trophoblast. Scale bar = 100 μ m.

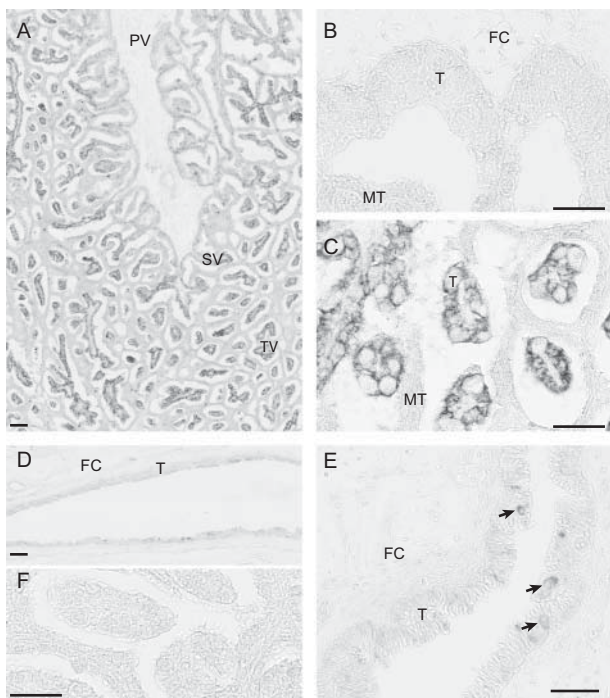


Figure 10 Immunohistochemistry of PAG2 protein in bovine placental (A, B, C and F) and interplacental (D and E) tissue sections at 220 days of gestation with the anti-PAG2 (L390) antibody. Panel A illustrates a global section of the placentome. Panel B illustrates the chorionic plate of the placentome. Panel C illustrates the internal secondary and tertiary villi. Panel F shows immunoneutralization of the anti-PAG2 antibody with the antigenic peptide. The anti-PAG2 antibody-labelled mononucleate cells of the placental villi and faintly labelled them in the intercotyledonary chorion. PV, primary villi; SV, secondary villi; TV, tertiary villi; FC, foetal connective tissue; MT, maternal tissue; T, trophoblast. (Arrows highlight mononucleate positive cells.) Scale bar = 100 μ m.

protein analyses. Highly specific PCR primers were designed and stringently selected so as to ensure that only the correct PAG transcript was amplified. Consequently, we deliberately chose not to report data concerning PAG9, PAG13, PAG14, PAG18 and PAG20 as there remained some doubt about their specific amplification. Another important objective of this work was to precisely determine the expression and localization of PAG during gestation at the protein level. Rabbit polyclonal antibodies were raised against synthetic peptides conjugated to KLH. During this study, antibody specificity was evaluated in various ways. The addition of an excess of blocking peptides or protein resulted in a loss of signal in both western blot and immunohistochemistry. No cross-reactivity between antibodies was reported. The fact that PAG are glycosylated proteins that could result in a multiple band pattern when running SDS-PAGE rendered validation of the antibodies more complex. Deglycosylation experiments demonstrated that antibodies recognized single bands of the expected molecular

mass corresponding to the polypeptide chains. A key element demonstrating antibody specificity was provided by the correlation between the levels of protein and mRNA expression. A lack of signal in negative control tissues known not to express the PAGs (such as the endometrium) provided an additional line of evidence for validation of the antibodies.

To our knowledge, no other study has specifically addressed the expression of numerous PAGs in both the intercotyledonary areas and cotyledon of the bovine placenta. Using RNase protection assays, one study (Green *et al.* 2000) reported that different PAG genes displayed different temporal patterns of expression during gestation, but it did not provide any information on the quantitative expression of transcripts and no data were collected with respect to the intercotyledonary chorion. Only two previous studies attempted to characterize and quantify the relative expression of PAG in the bovine placenta throughout gestation (Patel *et al.* 2004b, Telugu *et al.* 2009). Green's group (Telugu *et al.* 2009) established the differential expression profiles of PAG transcripts during gestation but solely

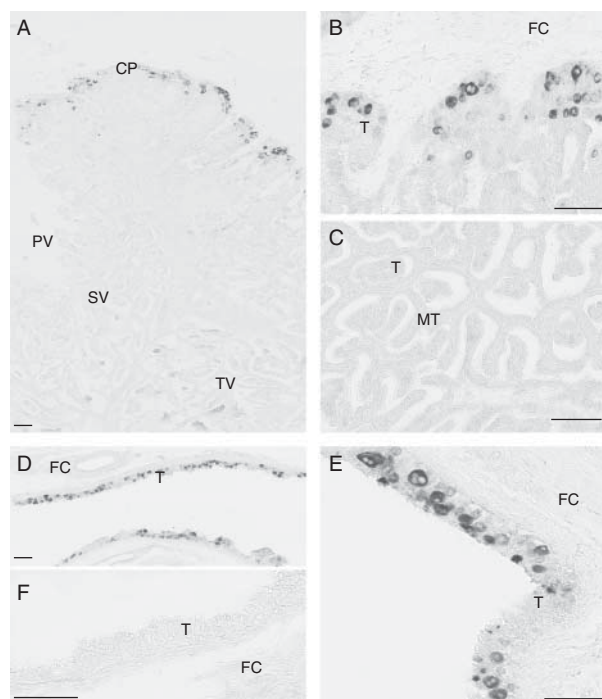


Figure 11 Immunohistochemistry of PAG11 protein in bovine placental (A, B and C) and interplacental (D, E and F) tissue sections at 220 days of gestation with the anti-PAG11 (L349) antibody. Panel A illustrates a global section of the placentome. Panel B illustrates the chorionic plate of the placentome. Panel C illustrates the internal secondary and tertiary villi. Panel F shows immunoneutralization of the anti-PAG11 antibody with the antigenic peptide. The anti-PAG11 labelled binucleate cells of the intercotyledonary chorion and chorionic plate of the placentome. PV, primary villi; SV, secondary villi; TV, tertiary villi; CP, chorionic plate; FC, foetal connective tissue; MT, maternal tissue; T, trophoblast. Scale bar = 100 μ m.

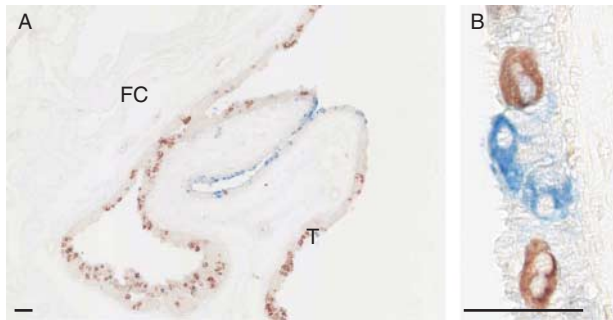


Figure 12 Localization of PAG1 and PAG11 proteins in bovine interplacentomal tissue sections at 220 days of gestation. Panel B is a higher magnification of the global view shown in panel A. Anti-PAG1 immunoglobulin was conjugated to alkaline phosphatase and visualized using Vector Blue alkaline phosphatase substrate and appeared in blue. Anti-PAG11 immunoglobulin was detected using a secondary biotinylated donkey anti-rabbit antibody revealed with an anti-biotin antibody conjugated to peroxidase. The immune complex was visualized using ImmPACT Novared peroxidase substrate and appeared in red. The anti-PAG1 and anti-PAG11 immunoglobulins identified distinct clusters of contiguous binucleate cells in the intercotyledonary chorion. FC, foetal connective tissue; T, trophoblast. Scale bar = 50 μm .

in the placental cotyledons, and only the ancient group of PAGs was examined. In our work, we were able to report that the expression of all PAGs increased as gestation progressed. PAG transcripts from the ancient group were more strongly expressed than those from the modern group. In addition, the most notable contribution of our work was to show that ancient PAGs were mainly expressed in the chorion of the intercotyledonary areas and to a lesser extent in the cotyledons. Despite the fact that the intercotyledonary chorion is considered not to play an essential role in placental function when compared with the cotyledon, the fact that ancient PAGs are expressed increasingly as gestation advances calls this into question. In the intercotyledonary chorion, the two most strongly expressed PAG transcripts were *PAG8* and *PAG10*, levels of which increased 30-fold between days 60 and 220 of gestation. One exception in the ancient group was *PAG2*, which was expressed predominantly in the cotyledon. Regarding *PAG2*, our findings were consistent with those of *Telugu et al. (2009)*. However, because their study was restricted to the cotyledon, a strict comparison of PAG expression profiles throughout the gestation between our results and those from Green's group (*Telugu et al. 2009*) would have been meaningless. With respect to *PAG1*, our results were in line with those of a previous report (*Patel et al. 2004b*), which showed a regular increase in *PAG1* with advancing gestation and a stronger expression in cotyledonary than in intercotyledonary regions. However, contrary to our investigation, which examined more PAGs belonging to both the phylogenetic groups, the study by *Patel et al. (2004b)* was restricted to analysing the expression of two modern PAGs in the intercotyledonary region.

In order to present our results, we classified PAGs into three groups as a function of the area where they were mainly expressed, rather than dividing them according to phylogenetic affiliation. Among the five ancient PAGs investigated, four were principally expressed in the intercotyledonary chorion and three of these (*PAG8*, *PAG10* and *PAG11*) exhibited increased levels of expression in line with gestation. As these PAGs were expressed at low and decreasing levels in the developing cotyledon, it could be suggested that their potential role is confined to the nonvillous chorion. The allocation of modern PAGs was less obvious. Among the modern PAGs supported by a substantial number of transcripts, three of them (*PAG1*, *PAG3* and *PAG15*) were mainly expressed in the cotyledon. However, it was only at later stages of gestation that their transcript levels increased dramatically. The other half of the modern PAGs were spread equally between the intercotyledonary chorion and the cotyledon.

In line with previous studies (*Xie et al. 1991, 1994, Zoli et al. 1991, Patel et al. 2004a, Klisch et al. 2006*), anti-PAG1 antibodies showed that the main PAG1 protein has an approximate molecular mass of 67 kDa and PAG1 has four potential sites for *N*-linked glycosylation (*Xie et al. 1991, 1995*). We demonstrated that the progressive deglycosylation of native PAG1 resulted in two deglycosylated intermediates and the fully deglycosylated protein at the molecular size expected for the polypeptide. Our findings indicated that PAG1 from placental tissue actually has four *N*-glycosylated sites. This was consistent with a previous report (*Patel et al. 2004a*) on bovine PAG from an explant culture-conditioned medium. As for PAG11, we demonstrated experimentally that the two *N*-glycosylation sites predicted by the amino acid analysis were actually glycosylated. The anti-PAG2 antibody revealed only one

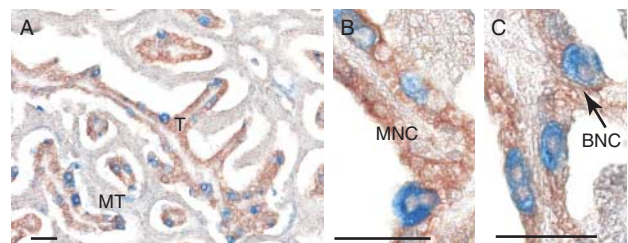


Figure 13 Localization of PAG1 and PAG2 proteins in bovine placental tissue sections at 220 days of gestation. Panels B and C are higher magnifications of the global view shown in panel A. Anti-PAG1 immunoglobulin was conjugated to alkaline phosphatase and visualized using Vector Blue alkaline phosphatase substrate and appeared in blue. Anti-PAG2 immunoglobulin was detected using a secondary biotinylated donkey anti-rabbit antibody revealed with an anti-biotin antibody conjugated to peroxidase. The immune complex was visualized using ImmPACT Novared peroxidase substrate and appeared in red. The double labelling identified PAG1 in binucleate cells and PAG2 in mononucleate cells of the placentome. MT, maternal tissue; T, trophoblast; MNC, mononucleate cell; BNC, binucleate cell. Scale bar = 50 μm . The arrow indicates a PAG1-positive binucleate cell.

unambiguous *N*-glycosylated site. The fact that PAG2 displayed a single *N*-glycosylated site, although six potential positions were predicted, could have been related to folding of the protein (Apweiler *et al.* 1999). Moreover, we suggest that PAG2 is weakly glycosylated because the protein is synthesized by mononucleate cells (see below) that might lack the specific glycosylation machinery evidenced in binucleate cells (Klisch & Leiser 2003). Global changes to PAG glycosylation have been reported during gestation (Klisch *et al.* 2006, 2008) but the precise protein involved has not yet been identified. As PAGs display different patterns of expression during gestation, and because we showed that their glycan residues differ in size, it could be suggested that PAG might to some extent be involved in global changes to glycosylation.

It is generally accepted that modern PAGs are only expressed in binucleate cells of the cotyledonary trophoblast, whereas the ancient group (exemplified by PAG2) is expressed in both mononucleate and binucleate trophoblastic cells of the cotyledons. Our results did not exactly fit this model. We showed that the ancient PAG2 was exclusively localized in mononucleate trophoblastic cells whereas PAG11, another ancient PAG, was exclusively localized in binucleate cells. Using *in situ* hybridization, Roberts' group was the first to suggest that PAGs from the ancient group are expressed in both mono- and binucleate cells, while modern PAG expression is limited to binucleate cells (Xie *et al.* 1994). However, when their experiments were performed, the diversity of the PAG family was unknown and, as pointed out later (Green *et al.* 2000), it is likely that the long probes commonly used for *in situ* hybridization lacked specificity and should have cross-reacted with both modern and ancient PAGs (Xie *et al.* 1994). Using immunohistochemistry, a more recent study supported the localization of ancient PAGs in both mononucleate and binucleate trophoblastic cells (Wooding *et al.* 2005). However, as suggested by the authors themselves, the precise specificity of the antibodies they used was not rigorously defined (Wooding *et al.* 2005). Their antibodies were raised using a protein fraction from affinity chromatography eluting at a neutral pH, which supposedly generated ancient PAGs (Green *et al.* 2005). However, to our knowledge, this has never been clearly demonstrated. Indeed, using mass spectrometry, it had been demonstrated (Green *et al.* 2005) that the antibodies raised against proteins eluting at a neutral pH only recognized PAGs from the modern group. We claim that the data inferred from our immunohistochemistry study were reliable because our antibodies were raised against specific peptides designed to differentiate PAGs. Both the two ancient PAGs we examined – PAG11 and PAG2 – were exclusively expressed in a single cell type. Our results therefore suggest that each PAG displays a unique cellular localization in either mononucleate or

binucleate cells. The question remains as to whether this pattern applies to all PAGs. Further studies are needed to examine this issue by including more PAGs from each phylogenetic group.

PAG1 was localized in binucleate cells of both the intercotyledonary and the cotyledonary chorion. Mononucleate cells expressing PAG2 were mainly detected in the cotyledon and only faintly in the intercotyledonary chorion. PAG11 was detected in binucleate cells of both the intercotyledonary and the cotyledonary chorion. However, unlike PAG1, which was detected in binucleate cells of the whole cotyledon, PAG11 was restricted to binucleate cells situated in the chorionic plate of the cotyledon. No binucleate cells expressing PAG11 were detected in the primary and secondary villi of the cotyledon. These results argue in favour of two populations of binucleate cells. Previous studies reported that the anatomical localization of binucleate cells in the ruminant placenta was associated with substantial differences in glycoprotein content (Lee *et al.* 1986, Wooding *et al.* 1996), but no evidence was provided regarding PAG synthesis. We addressed this issue by studying PAG1 and PAG11 co-localization. Our results demonstrated that two distinct cell populations synthesize PAG1 and PAG11, whereas no binucleate cells co-expressing the two proteins were detected. Moreover, in the intercotyledonary chorion, binucleate cells were observed as clusters of contiguous positive cells. Clumps of PAG1-positive binucleate cells were interspersed with those of PAG11-positive cells. These observations call into question the propagation of similar phenotypes in adjacent binucleate cells. Local factors might be suggested to explain differences in the gene expression pattern. Similar gene expression patterns would be observed for binucleate cells in the immediate vicinity while cells at a distant location would display another expression pattern. The way binucleate cells are generated should also be considered. It is generally accepted that binucleate cells originate from mononucleate cells by means of single acytokinetic mitosis (Wimsatt 1951, Wooding 1992, Wooding *et al.* 1994). Our results showing alternating aggregates of cells with similar phenotypes suggest that all the cells sharing a similar pattern of expression originated from a single cell. This is consistent with a previous suggestion (Wooding & Flint 1994) that any mononucleate trophoblastic cell can produce two cells, one of them leading to a binucleate cell through acytokinetic mitosis while the other remains as a mononucleate cell. Successive cell divisions of the latter will result in the generation of numerous binucleate cells sharing the same phenotype, as observed in our study.

Our findings highlight the important production of ancient PAG in the intercotyledonary trophoblast. This raises questions as to the role of proteins produced in such large quantities. Moreover, the evidence of PAG11 localization in binucleate cells suggests that it is possible

for an ancient PAG to reach the maternal blood circulation where none was previously evidenced. This suggestion is coherent in view of the ability of intercotyledonary binucleate cells to fuse with maternal cells as has been described in mouse deer presenting diffuse placentation (Wooding *et al.* 2007). This possibility implies putative functions for ancient PAGs, either within binucleate cells, during migration of the cells or in intercotyledonary areas of maternal tissues.

In summary, we have demonstrated that the levels of most of PAGs rise during gestation. Their expression patterns segregated into three distinct sets. PAGs from the ancient phylogenetic group were mainly expressed in the intercotyledonary chorion whereas modern PAGs were principally expressed in the cotyledon. One exception was PAG2, which is an ancient PAG, which was almost exclusively synthesized in the cotyledon. Moreover, we determined that PAGs were allocated to distinct trophoblastic cell populations. PAG2 was localized in mononucleate cells of the cotyledonary villi, PAG11 in binucleate cells of both the intercotyledonary region and the chorionic plate of the cotyledon and PAG1 in binucleate cells of both the intercotyledonary and the cotyledonary chorion.

Declaration of interest

The authors declare that there is no conflict of interest that could be perceived as prejudicing the impartiality of the research reported.

Funding

E Touzard was supported by a CIFRE (Convention Industrielle de Formation par la Recherche) scholarship from MESR (Ministère de l'Enseignement Supérieur et de la Recherche) via the ANRT (Association Nationale de la Recherche et de la Technologie).

Acknowledgements

The authors would like to thank Cyril Gonzalez and Michel Baratte for their technical assistance with animal management. They are grateful to Sylvaine Camous for fruitful discussions and Olivier Sandra for his pertinent advice. They also would like to thank Vicky Hawken for English language editing.

References

- Apweiler R, Hermjakob H & Sharon N 1999 On the frequency of protein glycosylation, as deduced from analysis of the SWISS-PROT database. *Biochimica et Biophysica Acta* **1473** 4–8. (doi:10.1016/S0304-4165(99)00165-8)
- Bridges PJ, Weems YS, Kim LM, Sasser RG, LeaMaster BR, Vincent DL & Weems CW 1999 Effect of PGF₂ α , indomethacin, tamoxifen, or estradiol-17 β on incidence of abortion, progesterone, and pregnancy-specific protein B (PSPB) secretion in 88- to 90-day pregnant sheep. *Prostaglandins & Other Lipid Mediators* **58** 113–124. (doi:10.1016/S0090-6980(99)00045-3)
- Butler JE, Hamilton WC, Sasser RG, Ruder CA, Hass GM & Williams RJ 1982 Detection and partial characterization of two bovine pregnancy-specific proteins. *Biology of Reproduction* **26** 925–933. (doi:10.1095/biolreprod26.5.925)
- Camous S, Charpigny G, Guillomot M & Martal J 1988 Purification of one bovine pregnancy-specific protein by high-performance liquid chromatography (HPLC). *Proceedings of the International Workshop on Maternal Recognition of Pregnancy and Maintenance of the Corpus Luteum, Jerusalem Israel, Kimron Veterinary Institute, Israel Abstr no.* 59.
- Chomczynski P & Sacchi N 1987 Single-step method of RNA isolation by acid guanidinium thiocyanate–phenol–chloroform extraction. *Analytical Biochemistry* **162** 156–159. (doi:10.1016/0003-2697(87)90021-2)
- Constant F, Camous S, Chavatte-Palmer P, Heyman Y, de Sousa N, Richard C, Beckers JF & Guillomot M 2011 Altered secretion of pregnancy-associated glycoproteins during gestation in bovine somatic clones. *Theriogenology* **76** 1006–1021. (doi:10.1016/j.theriogenology.2011.04.029)
- Dosogne H, Burvenich C, Freeman AE, Kehrli ME Jr, Detilleux JC, Sulon J, Beckers JF & Hoeben D 1999 Pregnancy-associated glycoprotein and decreased polymorphonuclear leukocyte function in early post-partum dairy cows. *Veterinary Immunology and Immunopathology* **67** 47–54. (doi:10.1016/S0165-2427(98)00215-3)
- Dosogne H, Massart-Leen AM & Burvenich C 2000 Immunological aspects of pregnancy-associated glycoproteins. *Advances in Experimental Medicine and Biology* **480** 295–305. (doi:10.1007/0-306-46832-8_34)
- Green JA, Xie S & Roberts RM 1998 Pepsin-related molecules secreted by trophoblast. *Reviews of Reproduction* **3** 62–69. (doi:10.1530/ror.0.0030062)
- Green JA, Xie S, Quan X, Bao B, Gan X, Mathialagan N, Beckers JF & Roberts RM 2000 Pregnancy-associated bovine and ovine glycoproteins exhibit spatially and temporally distinct expression patterns during pregnancy. *Biology of Reproduction* **62** 1624–1631. (doi:10.1095/biolreprod62.6.1624)
- Green JA, Parks TE, Avalle MP, Telugu BP, McLain AL, Peterson AJ, McMillan W, Mathialagan N, Hook RR, Xie S *et al.* 2005 The establishment of an ELISA for the detection of pregnancy-associated glycoproteins (PAGs) in the serum of pregnant cows and heifers. *Theriogenology* **63** 1481–1503. (doi:10.1016/j.theriogenology.2004.07.011)
- Hughes AL, Green JA, Garbayo JM & Roberts RM 2000 Adaptive diversification within a large family of recently duplicated, placentally expressed genes. *PNAS* **97** 3319–3323. (doi:10.1073/pnas.97.7.3319)
- Igwebuike UM 2006 Trophoblast cells of ruminant placentas – a minireview. *Animal Reproduction Science* **93** 185–198. (doi:10.1016/j.anireprosci.2005.06.003)
- Klisch K & Leiser R 2003 In bovine binucleate trophoblast giant cells, pregnancy-associated glycoproteins and placental prolactin-related protein-I are conjugated to asparagine-linked N-acetylgalactosaminyl glycans. *Histochemistry and Cell Biology* **119** 211–217. (doi:10.1007/s00418-003-0507-6)
- Klisch K, De Sousa NM, Beckers JF, Leiser R & Pich A 2005 Pregnancy associated glycoprotein-1, -6, -7, and -17 are major products of bovine binucleate trophoblast giant cells at midpregnancy. *Molecular Reproduction and Development* **71** 453–460. (doi:10.1002/mrd.20296)
- Klisch K, Boos A, Friedrich M, Herzog K, Feldmann M, Sousa N, Beckers J, Leiser R & Schuler G 2006 The glycosylation of pregnancy-associated glycoproteins and prolactin-related protein-I in bovine binucleate trophoblast giant cells changes before parturition. *Reproduction* **132** 791–798. (doi:10.1530/REP-06-0040)
- Klisch K, Jeanrond E, Pang PC, Pich A, Schuler G, Dantzer V, Kowalewski MP & Dell A 2008 A tetraantennary glycan with bisecting N-acetylglucosamine and the Sd(a) antigen is the predominant N-glycan on bovine pregnancy-associated glycoproteins. *Glycobiology* **18** 42–52. (doi:10.1093/glycob/cwm113)
- Kolaskar AS & Tongaonkar PC 1990 A semi-empirical method for prediction of antigenic determinants on protein antigens. *FEBS Letters* **276** 172–174. (doi:10.1016/0014-5793(90)80535-Q)
- Lee CS, Gogolin-Ewens K & Brandon MR 1986 Comparative studies on the distribution of binucleate cells in the placentae of the deer and cow using the monoclonal antibody, SBU-3. *Journal of Anatomy* **147** 163–179.

- Mialon MM, Camous S, Renand G, Martal J & Menissier F** 1993 Peripheral concentrations of a 60-kDa pregnancy serum protein during gestation and after calving and in relationship to embryonic mortality in cattle. *Reproduction, Nutrition, Development* **33** 269–282. (doi:10.1051/rnd:19930309)
- Patel OV, Takahashi T, Imai K & Hashizume K** 2004a Characterization of native and recombinant bovine pregnancy-associated glycoproteins. *Research in Veterinary Science* **77** 203–210. (doi:10.1016/j.rvsc.2004.05.003)
- Patel OV, Yamada O, Kizaki K, Takahashi T, Imai K & Hashizume K** 2004b Quantitative analysis throughout pregnancy of placental and interplacental expression of pregnancy-associated glycoproteins-1 and -9 in the cow. *Molecular Reproduction and Development* **67** 257–263. (doi:10.1002/mrd.20017)
- Rice P, Longden I & Bleasby A** 2000 EMBOSS: the European Molecular Biology Open Software Suite. *Trends in Genetics* **16** 276–277. (doi:10.1016/S0168-9525(00)02024-2)
- Sasser RG, Ruder CA, Ivani KA, Butler JE & Hamilton WC** 1986 Detection of pregnancy by radioimmunoassay of a novel pregnancy-specific protein in serum of cows and a profile of serum concentrations during gestation. *Biology of Reproduction* **35** 936–942. (doi:10.1095/biolreprod35.4.936)
- Szafarska B, Panasiewicz G & Majewska M** 2006 Biodiversity of multiple pregnancy-associated glycoprotein (PAG) family: gene cloning and chorionic protein purification in domestic and wild eutherians (Placentalia) – a review. *Reproduction, Nutrition, Development* **46** 481–502. (doi:10.1051/rnd:2006034)
- Telugu BP, Walker AM & Green JA** 2009 Characterization of the bovine pregnancy-associated glycoprotein gene family – analysis of gene sequences, regulatory regions within the promoter and expression of selected genes. *BMC Genomics* **10** 185. (doi:10.1186/1471-2164-10-185)
- Thompson IM, Tao S, Branen J, Ealy AD & Dahl GE** 2012 Environmental regulation of pregnancy-specific protein B concentrations during late pregnancy in dairy cattle. *Journal of Animal Science* **91** 168–173. (doi:10.2527/jas.2012-5730)
- Weems YS, Lammoglia MA, Vera-Avila HR, Randel RD, King C, Sasser RG & Weems CW** 1998 Effect of luteinizing hormone (LH), PGE₂, 8-EPI-PGE₁, 8-EPI-PGE₂, trichosanthin, and pregnancy specific protein B (PSPB) on secretion of progesterone *in vitro* by corpora lutea (CL) from nonpregnant and pregnant cows. *Prostaglandins & Other Lipid Mediators* **55** 27–42. (doi:10.1016/S0090-6980(98)00003-3)
- Weems YS, Lammoglia MA, Lewis AW, Randel RD, Sasser RG, Morita I & Weems CW** 1999 PGE₂ induces its own secretion *in vitro* by bovine 270-day placenta but not by 200-day placenta. *Prostaglandins & Other Lipid Mediators* **57** 189–205. (doi:10.1016/S0090-6980(99)00003-9)
- Weems YS, Bridges PJ, LeaMaster BR, Sasser RG, Ching L & Weems CW** 2001 Effect of the aromatase inhibitor CGS-16949A on pregnancy and secretion of progesterone, estradiol-17 β , prostaglandins E and F₂ α (PGE; PGF₂ α) and pregnancy specific protein B (PSPB) in 90-day ovariectomized pregnant ewes. *Prostaglandins & Other Lipid Mediators* **66** 77–88. (doi:10.1016/S0090-6980(01)00144-7)
- Wimsatt WA** 1951 Observations on the morphogenesis, cytochemistry, and significance of the binucleate giant cells of the placenta of ruminants. *American Journal of Anatomy* **89** 233–281. (doi:10.1002/aja.1000890204)
- Wooding FB** 1983 Frequency and localization of binucleate cells in the placentomes of ruminants. *Placenta* **4** 527–539.
- Wooding FB** 1992 Current topic: the synepitheliochorial placenta of ruminants: binucleate cell fusions and hormone production. *Placenta* **13** 101–113. (doi:10.1016/0143-4004(92)90025-O)
- Wooding FB & Flint APF** 1994 Placentation. In *Marshall's Physiology of Reproduction*, 4th edn, pp 230–466. Ed GE Lamming. London: Chapman and Hall.
- Wooding FB & Wathes DC** 1980 Binucleate cell migration in the bovine placentome. *Journal of Reproduction and Fertility* **59** 425–430. (doi:10.1530/jrf.0.0590425)
- Wooding FB, Morgan G, Brandon MR & Camous S** 1994 Membrane dynamics during migration of placental cells through trophoctodermal tight junctions in sheep and goats. *Cell and Tissue Research* **276** 387–397. (doi:10.1007/BF00306124)
- Wooding FB, Morgan G, Jones GV & Care AD** 1996 Calcium transport and the localisation of calbindin-D9k in the ruminant placenta during the second half of pregnancy. *Cell and Tissue Research* **285** 477–489. (doi:10.1007/s004410050664)
- Wooding FB, Roberts RM & Green JA** 2005 Light and electron microscope immunocytochemical studies of the distribution of pregnancy associated glycoproteins (PAGs) throughout pregnancy in the cow: possible functional implications. *Placenta* **26** 807–827. (doi:10.1016/j.placenta.2004.10.014)
- Wooding FB, Kimura J, Fukuta K & Forhead AJ** 2007 A light and electron microscopic study of the Tragulid (mouse deer) placenta. *Placenta* **28** 1039–1048. (doi:10.1016/j.placenta.2007.04.010)
- Xie SC, Low BG, Nagel RJ, Kramer KK, Anthony RV, Zoli AP, Beckers JF & Roberts RM** 1991 Identification of the major pregnancy-specific antigens of cattle and sheep as inactive members of the aspartic proteinase family. *PNAS* **88** 10247–10251. (doi:10.1073/pnas.88.22.10247)
- Xie S, Low BG, Nagel RJ, Beckers JF & Roberts RM** 1994 A novel glycoprotein of the aspartic proteinase gene family expressed in bovine placental trophoctoderm. *Biology of Reproduction* **51** 1145–1153. (doi:10.1095/biolreprod51.6.1145)
- Xie S, Green J, Beckers JF & Roberts RM** 1995 The gene encoding bovine pregnancy-associated glycoprotein-1, an inactive member of the aspartic proteinase family. *Gene* **159** 193–197. (doi:10.1016/0378-1119(94)00928-L)
- Xie S, Green J, Bixby JB, Szafarska B, DeMartini JC, Hecht S & Roberts RM** 1997 The diversity and evolutionary relationships of the pregnancy-associated glycoproteins, an aspartic proteinase subfamily consisting of many trophoblast-expressed genes. *PNAS* **94** 12809–12816. (doi:10.1073/pnas.94.24.12809)
- Zoli AP, Beckers JF, Wouters-Ballman P, Closset J, Falmagne P & Ectors F** 1991 Purification and characterization of a bovine pregnancy-associated glycoprotein. *Biology of Reproduction* **45** 1–10. (doi:10.1095/biolreprod45.1.1)
- Zoli AP, Demez P, Beckers JF, Reznik M & Beckers A** 1992 Light and electron microscopic immunolocalization of bovine pregnancy-associated glycoprotein in the bovine placentome. *Biology of Reproduction* **46** 623–629. (doi:10.1095/biolreprod46.4.623)

Received 8 April 2013

First decision 2 May 2013

Revised manuscript received 3 May 2013

Accepted 15 July 2013